



# KARST ROCK RELIEF OF QARA AND WHITE DESERT (WESTERN DESERT OF EGYPT)

## KRAŠKI SKALNI RELIEF V QARI IN BELI PUŠČAVI (ZAHODNA PUŠČAVA V EGIPTU)

Martin KNEZ<sup>1,2,3</sup>, Tadej SLABE<sup>1,2,3</sup>, Magdy TORAB<sup>4</sup> & Noura FAYAD<sup>5</sup>

### Abstract

UDC 551.3.053:552.54(620.21/.22)

*Martin Knez, Tadej Slabe, Magdy Torab & Noura Fayad: Karst Rock Relief of Qara and White Desert (Western Desert of Egypt)*

The karst rock relief clearly reveals the ways in which the karst surface and caves have been shaped and how they have developed. The oldest traces are the rock features of old karst caves, which were formed under climate conditions entirely different from the current ones, i.e., in the Pleistocene, and which have been dry for a longer period of time. Today, the wind is the prevailing factor in shaping the rock on the surface and in the karst of the White Desert near Farafra in particular, where we can witness the development of an entire range of wind rock features which helps us sort and classify them logically. However, in the wadis near the Qara Oasis a unique rock relief is forming, in which traces of water flow and dissolution of the rock under the sandy deposits are utterly predominant. The rainfall volume is low, however, the heavy rainfall events lasting short periods of time are enough to shape the less resistant rock. The rock features dominating the walls are co-shaped by dissolution and aeolian erosion. Crust forms on those parts of the rock surface that come in contact with water. The bare surfaces, on the other hand, are carved out by the wind. In the places where the crust has flaked off, the wind carves out cups.

**Keywords:** carbonate rock, rock relief, complexometry, Qara Oasis, White Desert (Farafra), Egypt.

### Izvleček

UDK 551.3.053:552.54(620.21/.22)

*Martin Knez, Tadej Slabe, Magdy Torab & Noura Fayad: Kraški skalni relief v Qari in Beli puščavi (Zahodna puščava v Egiptu)*

Kraški skalni relief tudi tokrat povedno razkriva način oblikovanja in razvoj kraškega površja ter jam. Najstarejše sledi so skalne oblike starih kraških jam, ki so se oblikovale v povsem drugačnih podnebnih razmerah od današnjih v pleistocenu in so že dlje časa suhe. Danes je prevladujoč dejavnik oblikovanja skale na površju veter in zlasti v krasu Bele puščave pri Farafri se razvija celoten nabor vetrnih skalnih oblik, ki služi tudi za njihovo smiselno razbiranje in razvrščanje. V vadijih pri oazi Qari pa se oblikuje svojevrsten skalni relief, v katerem povsem prevladajo sledi pretakanja vode in raztapljanja skale pod peščeno naplavino. Padavin je malo, a izrazitejša količina v kratkem časovnem obdobju je dovolj za oblikovanje slabše obstojne kamnine. Skalne oblike, kakršne prevladujejo na stenah, pa sooblikujeta korozija in vetrna erozija. Na delih skalne površine, ki jih dosega voda, nastane skorja. Gole površine pa dolbe veter. Na mestih, kjer se skorja odluči, veter izdolbe vdolbine.

**Ključne besede:** karbonatna kamnina, skalni relief, kompleksometrija, oaza Qara, Bela puščava (Farafra), Egipt.

<sup>1</sup> Research Centre of the Slovenian Academy of Sciences and Arts, Karst Research Institute, Titov trg 2, SI-6230 Postojna, Slovenia, e-mails: [knez@zrc-sazu.si](mailto:knez@zrc-sazu.si), [slabe@zrc-sazu.si](mailto:slabe@zrc-sazu.si)

<sup>2</sup> UNESCO Chair on Karst Education, University of Nova Gorica, Glavni trg 8, SI-5271 Vipava, Slovenia, e-mails: [knez@zrc-sazu.si](mailto:knez@zrc-sazu.si), [slabe@zrc-sazu.si](mailto:slabe@zrc-sazu.si)

<sup>3</sup> Yunnan University International Joint Research Center for Karstology, Xueyun road 5, CN-650223, Kunming, China, e-mails: [knez@zrc-sazu.si](mailto:knez@zrc-sazu.si), [slabe@zrc-sazu.si](mailto:slabe@zrc-sazu.si)

<sup>4</sup> Damanhour University, Faculty of Arts, Department of Geography, Abadia, Agriculture road, EG-5842001 Damanhour, Egypt, e-mail: [torab.magdy@gmail.com](mailto:torab.magdy@gmail.com)

<sup>5</sup> Damanhour University, Faculty of Arts, Department of Geography, Absom Alsharqia, EG-22821 Kom Hamada, El Beheira, Egypt, e-mail: [fayyadnoura43@gmail.com](mailto:fayyadnoura43@gmail.com)

## 1. INTRODUCTION

The rock relief with the most typical rock features clues us into the prevalent ways in which the karst surface of the studied areas has been shaped and how it has developed. It has never before been presented in these karst areas. We have presented mountain karst in dry environments (Al Farraj Al Ketbi et al., 2014; Audra et al., 2017). Reading the karst rock has once again made a major contribution to our understanding of the karst being formed on different carbonate rocks in diverse parts of the world (Knez et al., 2003, 2010, 2011; Debevec, 2012; Knez et al., 2012; Al Faraj Al Ketbi, 2014; Gutiérrez Domech et al., 2015; Knez et al., 2015, 2017, 2019; Slabe et al., 2016, 2021; Knez et al., 2020, 2022).

We began by studying the desert karst surrounding the Qara and Farafras oases. The karst in the Qara has never been researched before, as access to it is restricted. First of all, we present select features which we will attempt to combine into an overall image of the desert karst (Fayad, 2023).

In the Qara Oasis (Qarat Umm Al-Saghir Oasis) and the wider area, the formation and evolution of karst is significantly influenced by the different carbonate rock beds which have been incised by wadis (Figure 1). This paper focuses on a selected sample of smaller (tens of meters in diameter) wadis (Figure 2a) and their areas of contact with larger wadis (hundreds of meters in diameter). In some places, wadi basins are wide, indicating the presence of standing water at some point in the past.

The rock layers display different resistance to weathering and have been shaped by different processes, giving rise to the distinctive shape of the rocky perimeter of wadis and the occurrence of smaller and bigger solitary rocks and rock pillars with a unique rock relief (Figures 2b, 2c). The rock layers feature different carbonate contents and are of varying resistance.

By slowly dissolving the more resistant layers, it was through the action of water that this signature rock relief came about. Other layers are less resistant and quickly weather. They are more noticeably exposed to eolian erosion. They mostly break down into sand, which constitutes the prevalent land cover. The color of the landscape reflects the color of the weathered prevalent rock layer (Figure 2d). Where such layers predominate, the sloping walls are largely covered with sand (Figure 2e). The peaks are defined by the resistance of the individual layers. Where more resistant layers are underlain by less resistant rock, there occur overhanging walls (Figure 2f) and mushroom-like rock pillars (Figure 2g).

In the White Desert (Figure 3), the eolian rock relief is predominant, however, it does characteristically intertwine with traces of water and the resulting solidification of the rock surface into crust. We can discern a broad range of typical rock features. The rock relief noticeably dissects the surface of hills, cones, rock pillars and rocky ground, forming on the soft, white rock, chalk.



Figure 1: Lower parts of wadis, Qara.

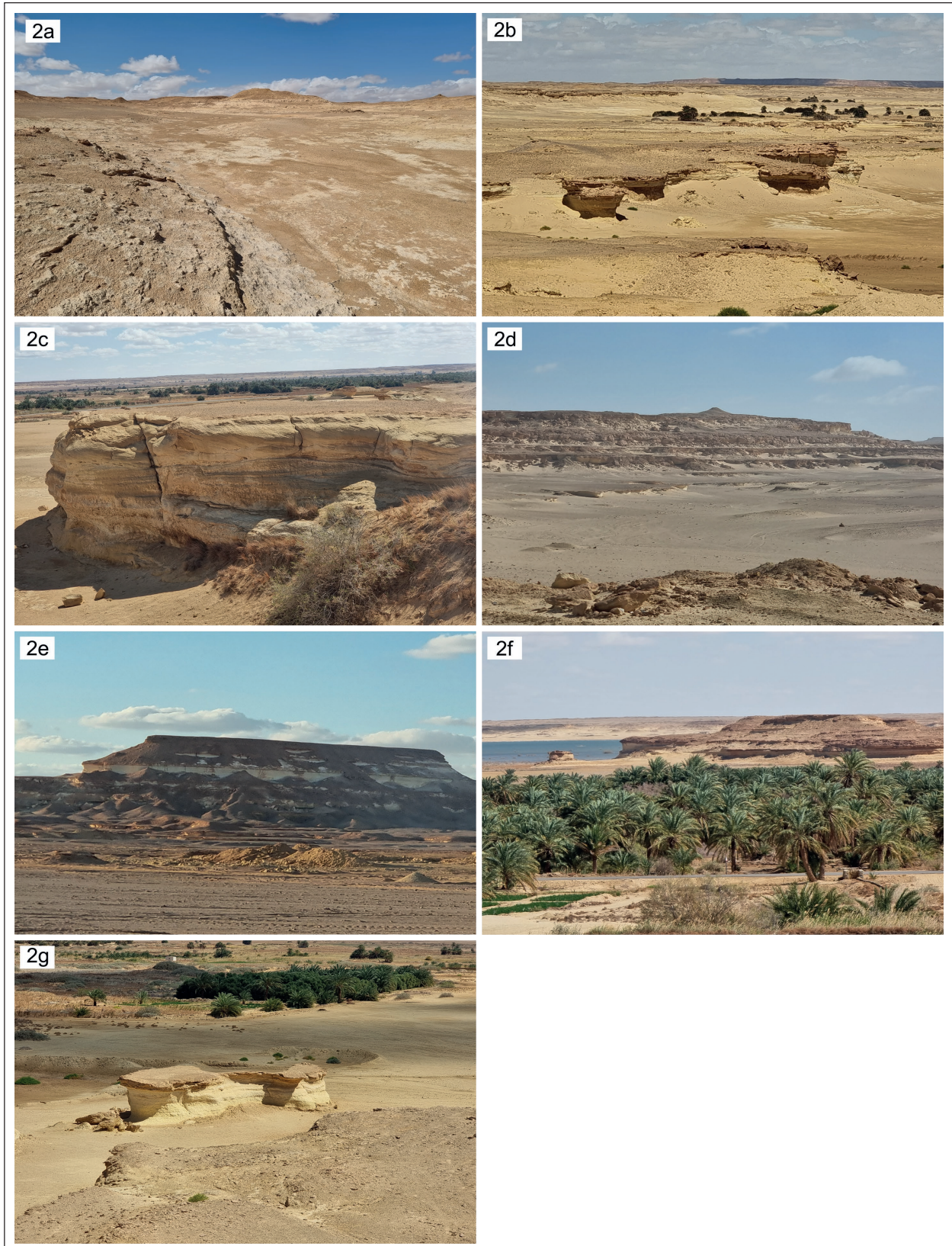


Figure 2: (a) Cross-section of the wadi, (b) Wall of the wadi, (c) Wall in different rock layers, (d) Wadi, (e) Wall covered by sand, (f) Harder layers of the rock on top, (g) Mushroom-like pillar.



Figure 3: White desert.

### 1.1. RESEARCH METHODOLOGY

We studied the rock relief and the rock features that comprise it. First, we identified the rock features in the field, then we discerned their shape and thoroughly mapped them. We linked their formation and shape with geological characteristics. The numerous photographs aided us in further researching the rock features. We then combined the studied karst features into a rock relief.

We defined the prevalent factors and the interaction of factors behind the formation of individual rock features. By combining these features into a rock relief, we attempted to determine the evolution of karst features.

In the Qara, we took 10 samples of rock at three layers' contacts: in two cases, we took the samples where we macroscopically noticed in the profile a clear contact between two layers, a major difference in rock compaction, a difference in porosity, and a difference in the degree of weathering of the rock. In one case, we took samples where we likewise noticed a clear contact between two layers, but the rock was macroscopically the same, i.e., the compaction of both layers, their porosity and degree of weathering were similar.

From 10 rock samples, 17 microscopic thin sections were prepared and examined by transmitted light. Prior to the microscopic examination, half of each sample was dyed with alizarin red dye (1,2-dihydroxyanthraquinone, known also as Mordant Red 11; Evamy & Sherman, 1962). Combining the observations with the results of the complexometric titration analysis, we were able to determine the properties of the rock.

In the Farafra region we took several samples; here we present 3 samples out of the 6 we took in Old White Desert.

All samples were ground and dried at 105 °C for 24 hours followed by cooling in a desiccator for 30 minutes prior to weighing (Table 1). We performed 6 complexometric titration analyses on 6 rock samples. We used two reference methods, determination of calcium oxide by EGTA and determination of magnesium oxide by DCTA (CEN, 2013). Both methods use photometric determination. Visual observation was performed. The indicator methylthymol blue changes color from pale green to pink in the case of calcium oxide, and from blue to gray in the case of magnesium oxide.

## 2. ROCK RELIEF OF RESISTANT CARBONATE ROCK LAYERS SUBJECT TO DISSOLUTION BY WATER IN THE WADIS OF QARA AND TRACES OF EOLIAN EROSION

### 2.1. QARA AREA

The Qara Oasis is located on the western edge of the Qattara Depression (Farouk et al., 2010), south of the city of Marsa Matrouh by about 198 km, and northeast of the Siwa Depression by 120 km (Figures 4, 5).

The topography of the Qara appears as an asymmetric depression, the eastern bottom of which is lower than its western parts.

The length of the depression from north to south is about 7.5 km, from east to west about 5.4 km, and its



Figure 4: Location of the Qara Oasis and White Desert (Western Egypt's Desert) (Google Maps, 2023).



Figure 5: Qara Oasis on the Western Edge of the Qattara Depression (Google Maps, 2023).

total area is about 45.7 km<sup>2</sup>. The western edge of the depression formed in the Middle Miocene carbonates (the Marmarica Formation; Figure 6) ranges between 5 meters in the north and 15 meters in the south a.s.l.; its eastern edge ranges between 32 meters in the north and 5 meters in the south. The deepest parts of the depression reach a level of 60 meters in the northeastern outskirts of the lake, where there are springs and wells (Farouk et al., 2010; Zaki et al., 2013).

The Qara consists of a depression that was carved into the carbonate rocks of Middle Miocene age during the Quaternary by several geomorphological factors:

1. The action of karst dissolving during humid periods of the Quaternary;
2. Mechanical weathering activity during dry periods

that led to the destruction of some landforms at the rock joints in particular;

3. The prevailing action of ablation by wind during the current drought periods and the transfer of weathered materials and sediments, which helped deepen the depression (Farouk et al., 2010; Zaki et al., 2013).

Despite the low rainfall, the surface rock relief, especially of the wadis and smaller caves, shows traces of water flow. The reason for that is the occasional heavier rainfall events.

A continuous denudational lowering of the surface of the area occurred through the action of ancient karst dissolution during the rainy periods of the Quaternary (El Awady et al., 2018). Moreover, the action of weathering

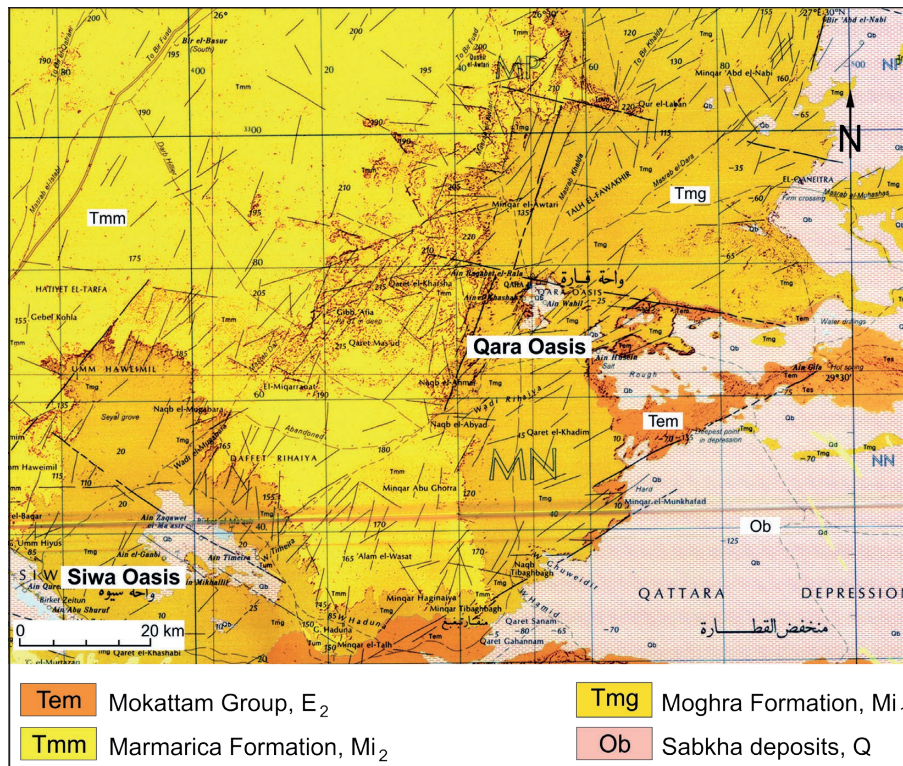


Figure 6: Cut of the geological map of Egypt, Siwa, 1:500.000 (Coy H.S.C., 1986).

processes and wind denudation helped erode the rocks of the area, leaving a group of scattered limestone hills that are gradually eroding due to the processes of weathering and wind sculpting during the current drought periods.

The geomorphological features in the Umm al-Saghir region can be divided into two types. Geomorphological features that were formed during the current dry periods and include the remaining limestone hills, such as the conical, domed, flat-topped, double-topped, oval, and mushrooms hills that spread out over the plains surrounding Lake Umm al-Sagheer and its marshes. There are also a number of wadis that cut the rocky edges surrounding the depression, especially from the western edge, which consists of Miocene limestones (the Marmarica Formation). The lowest parts of the depression are occupied by Lake Qara Umm al-Saghir, which derives its water from the hot springs that surround it, especially from the western side, where the water seeps towards the lowest parts of the region. On the shores of the lake, barriers and hooks have formed through the action of waves and the wind movement of sand grains. Sand grains gather around the assemblages of dry desert plants. Spread around the shores of the lake are the flats of Lake Sabkha, which dry up completely in the summer and a thin salt crust appears on them, mixed with sand and silt grains (El Awady et al., 2018; Farouk et al., 2010; Khalil et al., 2021; Thabet et al., 2013).

The second type of geomorphological features is the

forms created during past rainy periods, the most important of which are karst caves, most of which were affected by mechanical and chemical weathering processes, and the roofs of some of them have collapsed. It has been noted that the caves were formed by the effect of rainwater intrusion through the limestones of the Moghra and Marmarica formations, in addition to the influence of the geological weakness lines, especially the rock joints (Farouk et al., 2010). Smaller horizontal caves form under the hardened limestone crust at heights not exceeding one meter. The majority of such caves are found in the remaining limestone hills.

The annual average rainfall in Marsa Matrouh is 150 ml, and in Siwa only 50 ml. By calculating the distance between Umm al-Saghir and these two cities, it has been concluded that the annual average rainfall in Umm al-Saghir's neighborhood is about 75 ml (<https://www.meteoblue.com>) and maximum daily rainfall 28 mm, which is result of the Mediterranean climate.

## 2.2. GEOLOGY

At the fold of the stepped wall terrain, between the level of the central village and the top of the tens of meters tall step, the beds pinch out towards the south, forming a gentle incline that generally dips from the north to the south by 10 to 20°.

The diversely composed beds in some places continuously transition from one to the other, or the lateral

contacts between different beds have been obscured by the clasts of the upper layers. In places, either laterally or in the direction of the geologic column, the contacts between two beds of different textures and structures are more visible.

The outer edges of beds that outcrop into a stepped wall, where we can see their entire thickness in the stepped profile, are not vertical, but semicircularly rounded up the stepped incline.

The contacts between beds of different structures and textures, where we took rock samples directly below and directly above the contact, as described below, are not the kind of contacts where the upper layer is located on the surface over a larger area, thus fully exposed to the atmosphere, and where, conversely, the bottom layer is covered by the upper layer and thus protected against the impact of the atmosphere and karstification. Owing to the stepped beds making up the wall, we keep seeing new layers, from one meter to several meters apart, as we walk up the slope; therefore, all the parts of the beds that are not covered with younger layers, are evenly exposed to atmospheric impact. However, certain beds are

much more susceptible to weathering and karstification due to the loosely bound particles and higher porosity; these disintegrate more quickly into the predominantly original clasts, as they were before binding into a rock.

According to the geological map (Coy H.S.C., 1986; El Sisi et al., 2002), the wider area of the Siwa Oasis belongs to the Upper Eocene, to the Moghra Formation. The Moghra Formation consists of a continental to shallow marine clastic sequence including shale and white sandy carbonate beds, which are in some parts abundant with silicified wood. The uppermost carbonate layers transition to the Marmarica Formation which consists of fossiliferous shallow marine platform limestones with few marly intercalations.

### 2.2.1. MACROSCOPIC DESCRIPTION

Contact 1. The bottom layer (sample EGQ1, Table 1) is made up of very pale orange (10 YR 8/2; Munsell Rock-Color Chart, 2009) calcarenite, which is hard and compact within the layer; the clasts are tightly bound together (Figure 7a). However, on the surface it intensely disintegrates into the basic particles; hence, the somewhat hard

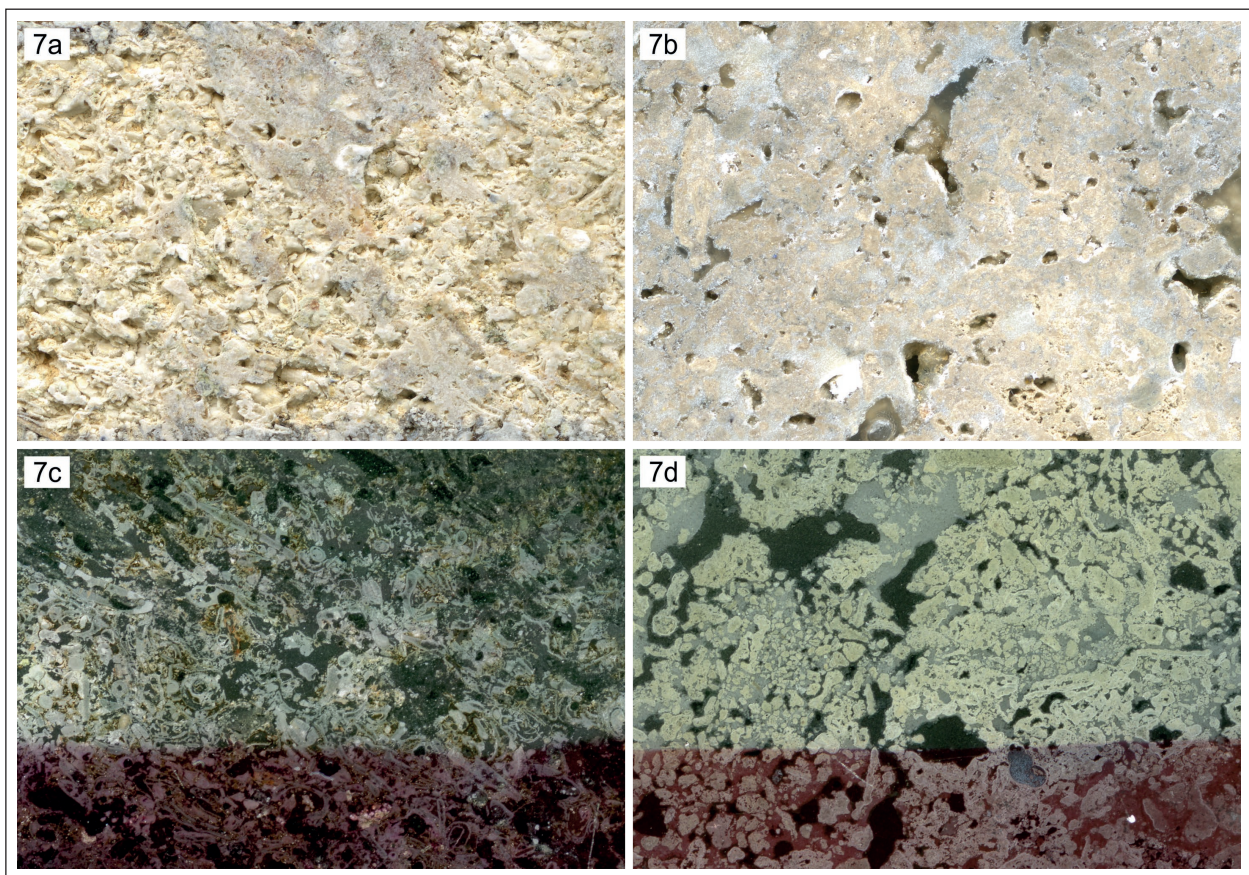


Figure 7: (a) Rock slice prepared for a thin section, sample EGQ1. Width of view is 4 cm, (b) Rock slice prepared for a thin section, sample EGQ2. Width of view is 4 cm, (c) Thin section of sample EGQ1. Lower half of sample was dyed in alizarin red dye. Width of view is 4 cm, (d) Thin section of sample EGQ2. Lower half of sample was dyed in alizarin red dye. Width of view is 4 cm.

layer in the area of the stepped wall, which is denuded and exposed to the atmosphere because of the inclined surface, transitions or re-disintegrates into fine-grained particles. Most of the grains in the rock are inorganic carbonate grains, mostly measuring around 1 mm in diameter. The rock particles are mostly spherical and either rounded or angular.

Visible among the grains are larger reflective crystal surfaces. We can rarely see several mm large pieces of unidentifiable fossil fragments in the rock, most likely molluscan. No cracks, calcite veins or other microtectonic characteristics are visible in the bed. Moreover, no diagenetic alteration is visible, however, we can see initial stages of binding and compaction. The fabric of sedimentary rock is very porous and has a great ability to transmit water. The upper layer (sample EGQ2, Table 1) differs greatly from the bottom one; it is composed of a darker (light gray, N7), more coarse-grained and much harder calcarenite (Figure 7b). The clasts in the rock measure up to a few mm in diameter and are more tightly bound together than in sample EGQ1. The grains in the rock are inorganic carbonate grains, mostly measuring a few mm in diameter, and angular. No fossil remains, cracks, calcite veins or other microtectonic characteristics are visible. The voids between the clasts have a higher cement content; there are fewer voids but they are larger (with a diameter of up to 10 mm) than in sample EGQ1. The rock is more resistant to weathering and atmospheric impact than the underlying layer. Rock porosity and the ability of water transmittance are much lower than in the underlying layer.

Contact 2. Contact 2 has similar characteristics as contact 1: less porous and more tightly bound clasts in the upper layer, and more porous and more loosely bound clasts in the bottom layer. The bottom layer of the pale yellowish orange (10 YR 8/6) calcarenite (sample EGQ3, Table 1) is rather hard and compact on the inside, but on the surface, and under the influence of the atmosphere, it disintegrates into the basic particles. In the rock we can observe mostly inorganic carbonate grains of varying sizes, from already weathered ones, smaller than 1 mm, to unweathered ones, measuring up to 1 cm in diameter. The rock particles are mostly prismatic and angular; some of them are also partially rounded and blade-like. Also visible in the rock are fossil fragments, some over 2 mm large, most likely from the Nummulitidae family and the bivalves group. No cracks, calcite or other microtectonic characteristics are visible in the bed; however, we can see initial stages of binding and compaction. The rock is very porous and has a smaller ability to transmit water than sample EGQ1. The upper layer of contact 2 consists of a lighter (grayish yellow, 5 Y 8/4), more coarse-grained, more com-

compact and harder calcarenite (sample EGQ4, Table 1), which is more resistant to weathering and atmospheric impact than the calcarenite in the underlying layer. The clasts in the rock measure from 0.5 cm to several cm in diameter. They are more tightly bound together than in sample EGQ3. The content of inorganic angular carbonate grains, with an average diameter of half a cm, in the rock has been estimated to roughly half; the other half comprises fossil remains from the Nummulitidae family and the bivalves group. There are a few empty spaces in the rock, measuring up to 1 cm<sup>3</sup>. Due to larger clasts oriented parallel, mostly bioclasts, the bed has a slate-like appearance in some places. Rock porosity and water absorption ability are lower than in the underlying layer.

Contact 3 is between two very similar layers of a fine-grained calcarenite; the bottom sample EGQ5 (Table 1), which is a pale yellowish orange color (10 YR 8/6), and the top sample EGQ6 (Table 1) of a grayish orange color (10 YR 7/4). The clasts in the rock, most of which do not exceed a few mm in size, are tightly bound; both rocks are quite hard and compact. No fossil remains are visible; only perhaps tiny fragments of the Nummulitidae family and the bivalves group here and there. No cracks, calcite or other microtectonic characteristics are visible in these two layers; however, we can see the initial stage of compaction. Both rocks are very porous, though without any larger voids; they have a high ability of water absorption and a low ability of water transmittance.

### 2.2.2. MICROSCOPIC DESCRIPTION

Contact 1. On account of the loosely bound particles in the rock and the macroscopically determined high porosity, we hardened sample EGQ1 with Araldite before making the thin section. A major difference in the composition of both rocks at the contact is also visible in the microscope slides. The bottom layer (sample EGQ1, Figure 7c) is made up of micritized carbonate intraclasts with diameters from 0.5 to 1 mm, and of mostly up to 2 mm longitudinally elongated bioclasts (mainly algae) and numerous fragments of various bioclasts. There is virtually no cement; only exceptionally do we see drusy calcite spar among the rock clasts. The intraclasts and bioclasts are carbonate, while some of the micritized clasts are of non-carbonate origin, namely in the places where we were unable to determine staining with alizarin and based on the complexometric titration analyses. A high percentage of the dolomite belongs to bioclasts. Mechanical compaction is well visible in the rock on the damaged larger elongated bioclasts. Regardless, the porosity of the rock, which can be classified as rudstone, is very high, estimated at a minimum

of 70%. The upper layer (sample EGQ2, Figure 7d) is made up of intraclasts, mostly measuring from 45  $\mu\text{m}$  to 0.5 mm in diameter, exceptionally up to 1 mm. No bioclasts are visible in the rock; however, there are a few peloids. The clasts are tightly bound together with microparite and druzey calcite spar cement. The crystals of the druzey calcite spar cement, with diameters between 45 and 200  $\mu\text{m}$ , are well visible on the inside of the numerous fenestrae. The latter are partially and, in some places, fully filled with druzey calcite spar. The fenestrae that are not fully filled have diameters between 0.1 and 2 mm, but mostly around 0.7 mm. The porosity of the carbonate rock of the grainstone or packstone type has been estimated at about 5 to 10%.

Contact 2. Here too, on account of the loosely bound particles in the rock, we hardened the bottom layer with Araldite before making the thin section. Very similar differences in the composition of both rocks, as described in the case of contact 1, are also visible in the microscope slides of contact 2. The bottom layer (sample EGQ3) is made up of carbonate intraclasts and many larger bioclasts. Some of the intraclasts are smaller, with diameters up to 0.1 mm; a small number of them are larger and of irregular shapes, with diameters up to 1.4 mm. The majority of bioclasts, which represent the dolomite part of the rock (some reaching over 4.5 mm in the longitudinal direction), belong to the Nummulitidae family and algae. The cement laterally and seemingly randomly transitions from micrite to sparite, taking up about 20% of the rock. Alizarin did not stain the dark fine-grained cement in many places; we therefore assume that a part of the cement is non-carbonate and makes up the insoluble residue. No major traces of compaction are visible. The porosity of the grainstone- or packstone-type rock has

been estimated at about 60 to 70%. The upper layer (sample EGQ4) is likewise made up of intraclasts and some extraclasts, both of which are mostly micritized, and of bioclasts. The intraclasts and extraclasts are larger in size, with an average diameter between 0.9 and 1.8 mm, and are tightly cemented together. The cement is micrite and sparite. Mechanical compaction is well visible. Most of the bioclasts from the Nummulitidae family, as well as the algae and corals, are broken and their pieces have been displaced, in some places by 0.5 mm. Much like in contact 1, porosity is lower in the upper layer and has been estimated at about 15 to 20%.

Both layers of contact 3 are almost identical, both in the macroscopic and microscopic view. They are made up of intraclasts of different sizes, ranging from 0.1 mm to 0.6 mm; most of them measure around 0.3 mm in diameter. There are no bioclasts in the layers. The cement is sparite and micrite, in some areas laterally dolomite, and of non-carbonate origin. Compared to the previous layers, the rock is highly compacted. Porosity has been estimated at 10 to 15%.

### 2.2.3. COMPLEXOMETRIC TITRATION ANALYSES

The samples of contact 1 are almost entirely carbonate, with a total carbonate content between 91 and 94% (Table 1). The bottom layer contains a slightly higher amount of insoluble residue than the upper layer. A major difference between both layers is the calcite-dolomite ratio. Whereas over 50% of the rock underneath the contact is made up of calcite and as much as 40% of dolomite, almost 90% of the rock above the contact is made up of calcite.

The samples of contact 2 have a slightly lower total carbonate content, with the bottom layer containing just under 83% and the upper layer almost 90%.

Table 1: Complexometric analyses of rock samples (granulation < 0.25 mm, dried 24h at 105 °C); samples from Qara (EGQ1 to RGQ6) and samples from White Desert (EGF21 to EGF23).

Laboratory designation of the sample	Rock sample	CaO (%)	MgO (%)	Calcite (%)	Dolomite (%)	CaO/MgO	Total carbonate (%)	Insoluble residue (%)
V- 53/23	EGQ1	28.65	19.31	51.13	40.39	1.48	91.52	8.48
V- 54/23	EGQ2	49.92	2.03	89.10	4.25	24.59	93.35	6.65
V- 55/23	EGQ3	26.38	17.07	47.08	35.71	1.55	82.79	17.21
V- 56/23	EGQ4	30.48	16.75	54.40	35.04	1.82	89.44	10.56
V- 57/23	EGQ5	22.23	15.37	39.68	32.15	1.45	71.83	28.17
V- 58/23	EGQ6	24.41	16.54	43.57	34.60	1.48	78.17	21.83
V- 59/23	EGF21	33.79	17.21	60.31	36.00	1.96	96.31	3.69
V- 60/23	EGF22	53.81	0.99	96.04	2.07	54.35	98.11	1.89
V- 61/23	EGF23	54.10	1.01	96.56	2.11	53.56	98.67	1.33

The bottom layer contains just over 17% of insoluble residue, and the upper layer just over 10%. Much like in contact 1, the bottom layer has a lower calcite content than the upper layer, while both layers have the same dolomite content.

The samples of contact 3 are very similar; they have a similar total carbonate content, and a similar calcite, dolomite and insoluble residue content.

### 2.3. ROCK RELIEF

Occurring in various sizes, the smaller wadis join the bigger ones in dendritic patterns, occasionally – when smaller wadis drain into the larger ones from the flank – creating steep parts of water bed.

Distinct rock features, which came about due to the dissolution of the rock, can be made out in the harder (e.g., samples EGQ2, EGQ4), more resistant and more calcite-rich rocks, and in the contact with the less resis-

tant carbonate rocks (e.g., samples EGQ1, EGQ3) which disintegrate into very fine, original particles (Figure 8). Their different compositions (with varying sizes of clasts and degrees of porosity) are also reflected in the rock relief. Fossils are also visible (Figure 9a). Such rock stratification can occur in repetitive sequences, where harder layers with traces of dissolution and the disintegrating layers overlying them can be stacked on top of each other. The more resistant layers are rounded and either protrude from the higher wall or form stepped walls (Figure 2b), forming the resistant top of the karren. They become exposed over time by the action of wind and water. As they are more resistant and solid, these layers often end up being the wadi's bed over prolonged periods. Subject to periodical water flows in varying amounts, the rock relief shows traces of sand being carried to and away, of being covered and then exposed again.

Subsediment rock features are formed as water per-



Figure 8: Rock relief of the wadi. a. subsediment cup, b. subsediment rock pillar, c. large solitary rocks, d. half-cup notches, e. half-cup notches, f. subsidiary channels, g. small half-bell, h. smaller and bigger steps, i. subsediment steps, j. larger channels, k. channels.

colates through the detritus of the upper disintegrating layer, thereby dissolving the lower layer, and on sloping surfaces as water is drained away. Various subsediment cups are formed on horizontal or gently sloping surfaces, whereas subsediment channels are formed on inclined surfaces.

On the rock, which is covered with sand in places, subsediment cups are formed, sometimes next to each other (Figures 8a, 9b), and subsediment channels with a diameter ranging from 10 cm to several meters and with small stone pillars between them. This applies to the upper parts of the karren. In sandier rock layers, there are irregularly shaped subsediment cups with outstanding ragged edges (Figure 9c), which are either the result of the dissolution and consolidation of the sandy carbonate rock or of the frequent, partial or complete, covering and exposing of the surface. Under the same conditions, a surface which is composed of less resistant, sandier rock, and is slightly more soluble, will become dissected by tiny, centimeter-sized cups (Figure 9d). Such surfaces also contain larger subsediment cups. Such cups also form beneath the steep sections of cliffs, with channels leading down to them. Sand is deposited in them by water and wind, and the rock underneath dissolves more efficiently and over longer periods. Between them, small subsediment rock pillars form. In some places, they make up veritable stone forests (Figures 8b, 9e) with ten-centimeter-tall pillars that take a mushroom shape, provided that their top layers are more resistant to corrosion and erosion. They protrude from the mainly sand-covered surface.

They are a common feature of the wadi's banks that divert water to the bottom, which we will proceed to describe below. Large solitary rocks (Figures 8c, 9f) stand out between, and sometimes within, the relatively dense network of smaller and shallower wadis.

At the end of the layer which terminates in a stepped wall are the uniquely shaped tops of rock steps (Figure 9g). Below the step, a subsediment longitudinal notch has formed, which is dissected by half-cup notches on the outflow side (Figures 8d, 8e, 9g). They catch water from the sand that covers the notch. The largest channels are also, at least periodically, subsedimentary (Figures 8f, 9h) as their bottom is covered by sand. Also formed subsedimentary are the mouths of channels which drain away the water coming down the step (Figure 9g); the water runs down the channels in the steep part of the wall between the ledges (Figure 9i). As a result, funnel-like notches have also formed on the occasionally sand-covered top edge of the rock ledge (Figure 9j). There are also small half-bells in the lower part of the steeper wall sections, which are occasionally covered by sand (Figures 8g, 9k). Channels also form on overhanging sections un-

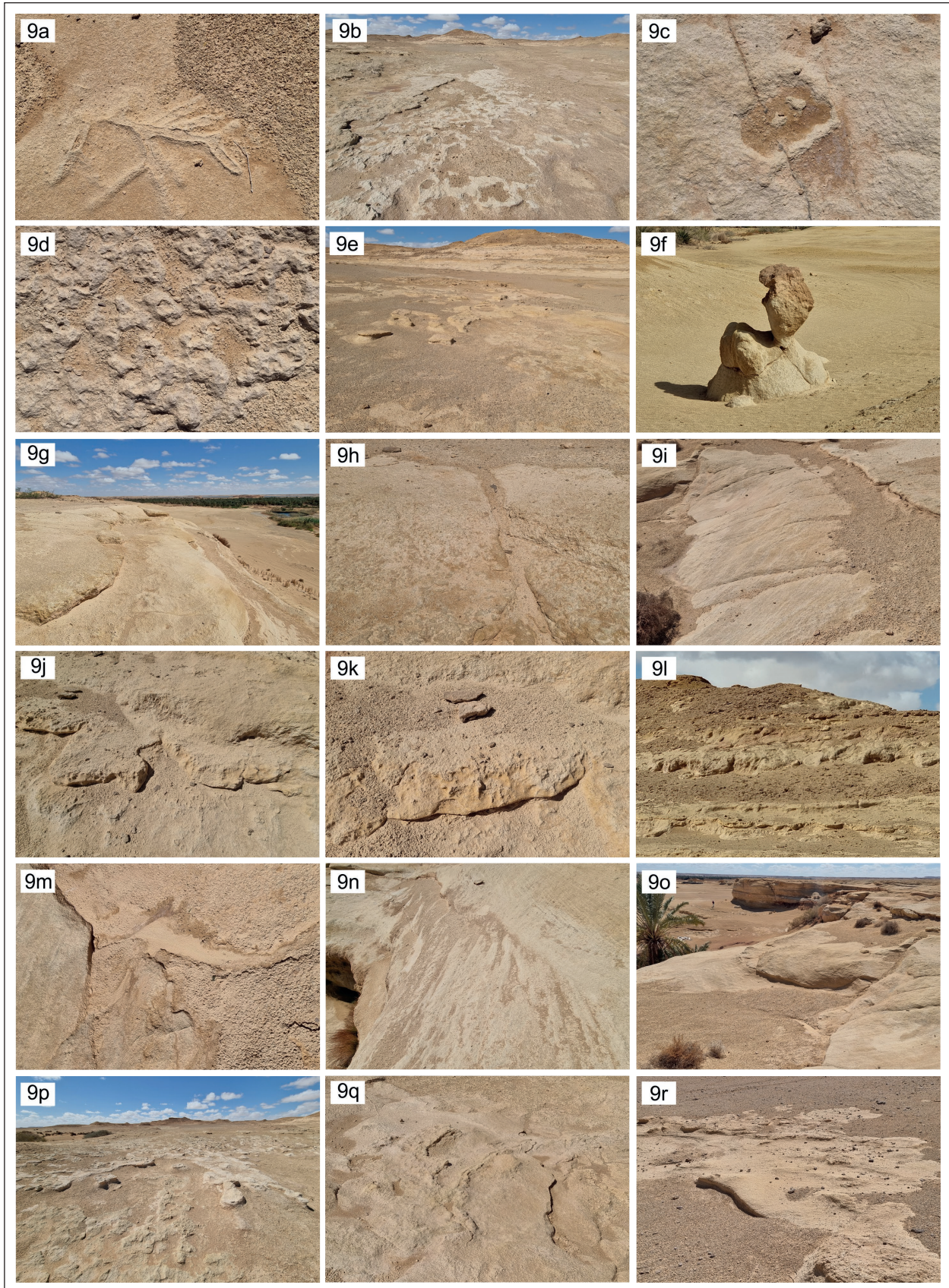
der the disintegrating layer that extends to the edge of the wall. This is also true of the rock relief of the steep parts in the bed. A semicircular longitudinal notch may also form at the lower sections of steep edges (Figures 8d, 9l). Some channels (Figure 9m) that have formed under small springs between rock layers are also subsedimentary.

Smaller and bigger steps (Figure 8h) have also formed on the sloping surface as a result of the water creeping down the surface, carrying and depositing sand. Underneath, dissolution occurs slightly faster and over extended periods (Figure 9n). A step has also formed at the contact of the upper, harder layer, which dissolves more slowly, and which covers and protects the slightly less resistant lower layer (Figure 9o). A channel has formed in its wall, leading to a subsediment cup in the lower layer.

At the bottom of the shallow wadis, in which sand is transported by water and partly wind, and which are usually sand-covered in places, a typical rock relief can be made out (Figure 9p). It is dominated by large (with a diameter of up to one meter) half-cup notches, which are semicircular in shape on the inflow side and open on the outflow side. In many instances, they occur in tiers, one on top of the other (Figures 9p, 9q). There are also larger (meter-sized) subsediment steps (Figures 8i, 9r) which are occasionally bare and feature steep inflow edges. On the lower part of the steep edges, subsediment longitudinal notches (Figures 9r, 9s) form at the bottom of the bed or the banks, which are traces of the frequent changes in the level of sand that covers the bottom of the wadi. In the lowest parts of the bed, larger channels (Figures 8j, 9t) have formed, which also develop from or at the bottom of subsediment cups (Figure 9u). The bottom of the wadi is often completely covered or exposed to varying degrees. Water also runs in from the sides (Figures 8k, 9v), as is noticeable in the rock forms (Figures 8k, 9w). The rocky wadi bottom is also eroded and reshaped by the water and the sand it carries. The most exposed parts are therefore relatively smooth and dissected by shallow cups (Figure 9x). Here, the small rock protrusions that characterize the banks of the wadis and the higher parts of the karren described above are not present. Only larger protrusions (Figure 9y, center) can be seen.

On the bare rock, especially in the steeper sections, channels have formed that drain water from the layers, which break up into sand (Figure 9z), and the bedding plane caves. There are also cases where the water creeping down the bare rock forms channels. On the gently sloping sections, these are partly or periodically covered with sand.

The overhanging parts of the higher walls are dis-



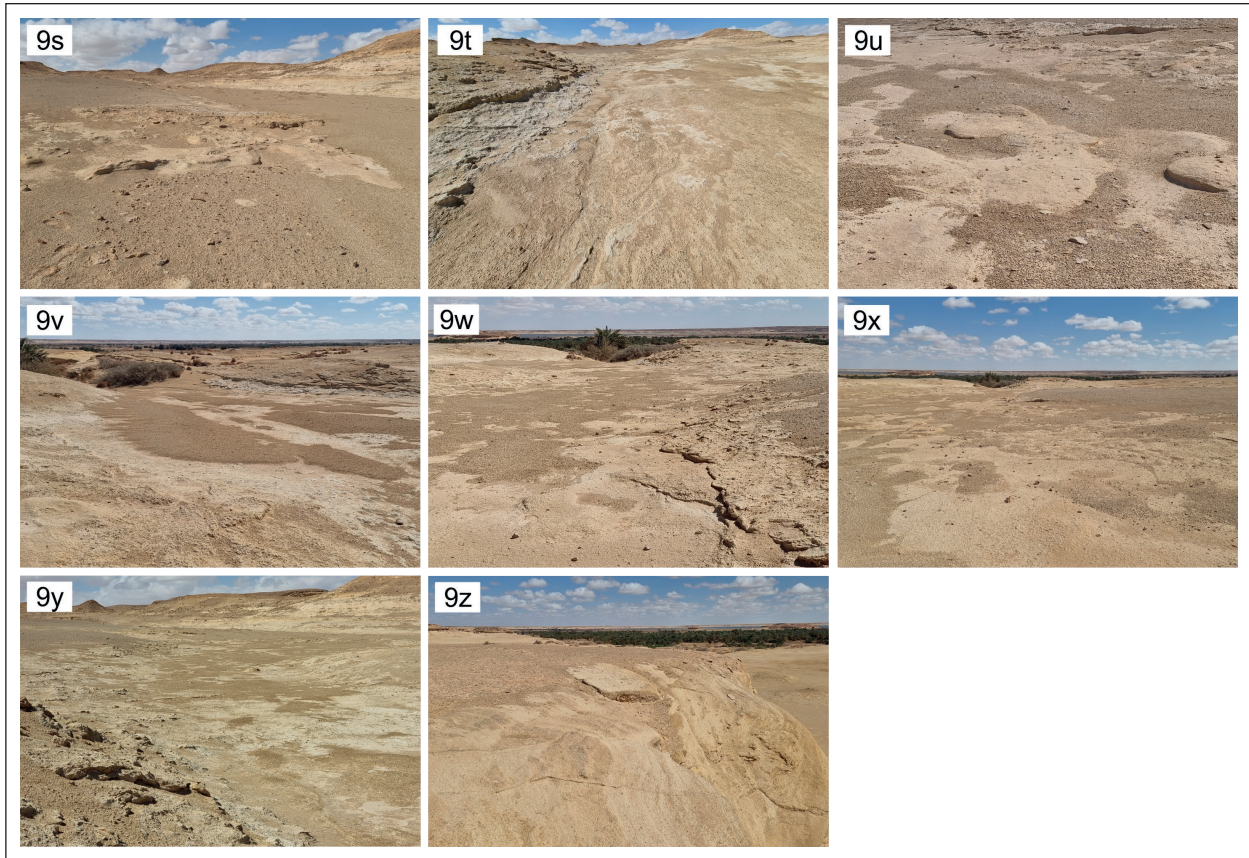


Figure 9: (a) Fossil in the rock. Width of view is 45 cm, (b) Subsediment cups. Width of view is 3.5 m, (c) Subsediment cup with a higher edge. Width of view is 1 m, (d) Small subsediment cups. Width of view is 25 cm, (e) Small rock pillars, (f) Rock pillar. Width of view is 5 m, (g) Stepped wall at the end of the wadi, (h) Subsediment channel. Width of view is 3 m, (i) Subsediment funnel-like notches and channels. Width of view is 7 m, (j) Subsediment funnel-like notch. Width of view is 1.5 m, (k) Subsediment half-bell. Width of view is 1.5 m, (l) Longitudinal subsediment notch, (m) Channel under a small spring. Width of view is 1.5 m, (n) Small steps on the steep wall. Width of view is 6.5 m, (o) Longitudinal notch between the less resistant and more resistant rock layer. Figure 9p: Half-cup notch, (q) Half-cup notches in a tier. Width of view is 5 m, (r) Large subsediment steps. Width of view is 7 m, (s) Longitudinal subsediment notch, (t) Large channel on the bottom of the wadi. Width of view is 7 m, (u) Subsediment cups and channel. Width of view is 6 m, (v) Traces of water flowing from the sides of the wadi. Width of view is 25 m, (w) Traces of water flowing from the sides of the wadi, (x) The most exposed parts of the wadi bottom with shallow cups, (y) The most exposed parts of the wadi bottom with shallow cups and a large protrusion, (z) Channels on the rock edge.

sected by tiny cups, a few centimeters in diameter, which connect into a network. They appear to be of subsediment origin, some of them partially infilled and covered by a crust of solidified solution overlying the lower, occasionally covered, overhanging parts of the wall (Figure 10a). Located above them are wider wall channels (Figure 10a), also subsedimentary judging from their form, which were later reshaped by creeping water. Above ground, however, large longitudinal notches have formed, most of them longitudinally cup-shaped (Figure 10b), which can be traced to the steady levels of sand surrounding the rock.

The subsediment bedrock has a relatively smooth surface, whereas the upper parts of the mostly bare rock, which are only occasionally covered with fine sand, are

coarse, depending on the composition of the rock (Figure 10c).

The karren are most prominently perforated along the bedding planes (Figures 2d, 2e). The smallest cavities have a diameter of about one centimeter (Figure 10e). Typically, the caves are relatively wide (several meters) and low (Figure 10f).

Only the largest old caves (Fig. 11) are accessible. In some places, more pronounced central pipes have formed, which might occur as ceiling channels where the ceiling is made up of a more highly soluble rock. Conversely, a bottom channel is formed if the water cuts into less resistant rock overlain by a more resistant layer. In some places there are springs of water on the edges of the rock walls, and underneath them epiphreatic caves.

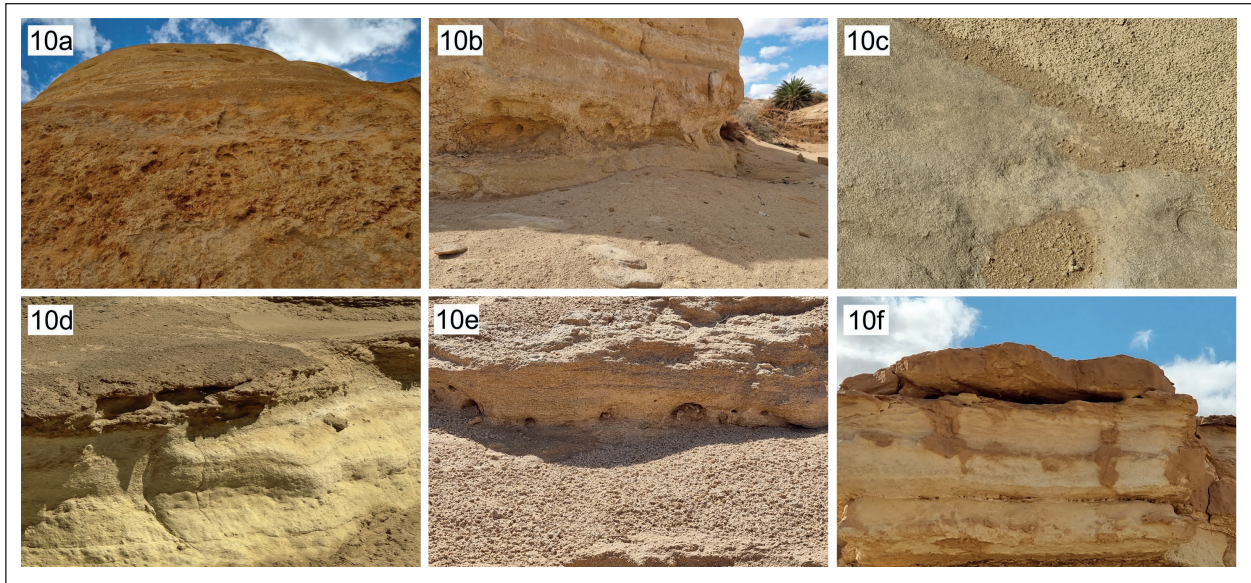


Figure 10: (a) Overhanging wall with channels. Width of view is 4 m, (b) Overhanging wall with a longitudinal notch and large cups, (c) Trace of rock composition on its surface. Width of view is 30 cm, (d) Wind scallops. Width of view is 8 m, (e) Small hollows. Width of view is 5 m, (f) Small caves along bedding planes. Width of view is 7 m.

Water flowing out of the bedding-plane recent forming caves carves out channels in the wall through different layers of rock, including those that quickly disintegrate on the surface.

In Qara the sandy, less cohesive and thus less resistant rocks are eroded by the wind. This results in rounded surfaces and the formation of longitudinal notches next to them, which are dissected by large and shallow (several tens of centimeters or a meter or more

across) wind scallops (Figure 10d). Their surface is further dissected into small cups (Figure 9r), which are largely linked to porous layers and narrower notches, weak spots in the structure and the fissuring of the rock, and into smaller protrusions which are in fact parts of a more resistant rock. Longitudinal notches also form along the contact within the layers. The rock disintegrates into sand, which is picked up by the wind and deposited on the karst surface.



Figure 11: Entrance into the cave.

### 3. EOLIAN EROSION IN THE KARST OF THE WHITE DESERT IN FARAFRA

#### 3.1. WHITE DESERT, FARAFRA

The floor of the depression (Figure 3) exposes a large expanse of flat-lying Cenomanian fluvial sandstones. Around the margins these pass upwards into the terrestrial to marine transitional clastic beds well known for their vertebrate fauna (Slaughter & Thurmond, 1974; Stromer, 1936). This is followed by a carbonate bed called the El Heiz Bed (Said, 1990). Above this, a mixed lithological section of dolomites and clastics, the Hefhuf Formation, can be traced around much of the rim of the depression, but is absent in the part of the northern area where pre-Middle Eocene erosion has breached the crest of the dome down to the Cenomanian clastics. Maastrichtian to Danian age chalky limestone or Farafra chalk (Coy H.S.C., 1987; Issawi, 1972; Plyusnina et al., 2016) is present in the southwest from the oasis below the Eocene carbonates.

In the area of Farafra rainfall amounts to merely 11.8 mm (El-Marsafawy et al., 2019).

#### 3.2. GEOLOGY

We took several samples of rock in the area of Crystal Mt., Aqaba, and Old and New White Deserts (all locations are up to a few tens of km northeast from the Farafra Oasis). Presented below are three samples out of the six we took in Old White Desert: a sandstone sample and two chalk samples. On the geological map (Coy H.S.C., 1987) the rock is shown as white massive neritic chalk and chalky limestone (the Khoman Formation) which interfingers with submarine fan deposits of yellowish carbonate-bound siltstone and sandstone intercalated with clay, known as the Dakhla Formation.

##### 3.2.1. MACROSCOPIC DESCRIPTION

The depressions between the smaller rocky hills consist of a brown ochre (10 YR 6/6 and 10 YR 5/4; Munsell Rock-Color Chart, 2009) sandstone (sample EGF21; Table 1). The sandstone is carbonate, which we were surprised to discover after performing an acid test; it is fine-grained and many particles with a smooth, reflecting plane are visible on its surface. On the broken surfaces we can feel that the grains are angular. The rock is completely homogeneous, consisting of macroscopically identical grains; no gradation is visible in the profiles, the rock is uniform and hard: the particles are tightly bound together. No porosity was visible macroscopically; we noticed considerable porosity only after examining the rock with a field magnifier and later, when processing the samples in the laboratory. Exceptionally, we see intercalations in the rock – spherical sinedi-

mentary white and carbonate and brownish-red non-carbonate intraclasts, mostly measuring up to a few cm in diameter, which are believed to have originated from iron-rich paleosol (ferricrete) horizons (Catuneanu et al., 2006).

In some places on the eroded rock surface, smoothed by eolian erosion, there are many dissolved/broken-off non-carbonate reddish-brown clasts, most likely also due to the weathered younger layers, which have been carried away by the wind.

The small rocky hills, located next to each other in some places or alone on a plain at the edge of such groups, are composed of pure white fine-grained carbonates (white, N9); the rock is chalk (samples EGF22, EGF23, Table 1). There are hardly any larger clasts visible on the surface of the rock; only exceptionally are there fragments of various bioclasts, mostly measuring up to 10 mm in diameter, distributed across horizons, several meters thick. In these horizons we notice different bivalves (Figure 12) here and there; in many places, they protrude from the rock by several cm. The contacts between the sandstones that make up the depressions and between the chalk that makes up the small rocky hills are mostly obscured by the sand from the weathered sandstone.

##### 3.2.2. MICROSCOPIC DESCRIPTION

Due to the loosely bound particles in the rock, we hardened all the samples with Araldite before making the thin section. The brown ochre sandstone (sample EGF21) is composed entirely of almost equal-sized carbonate grains of calcite and dolomite. Individual sections of the rock can be identified as having a dolomite mosaic idiomorphic texture with euhedral unimodal crystals. The average grain size is between 0.2 and 0.3 mm; only individual grains reach a diameter of 0.5 mm. The grains touch and overlap; cement that would additionally bind individual clasts together is not visible. Most of the grains are heavily micritized. There is no visible compaction; the grains are not damaged, nor in any way deformed. There are no bioclasts or other types of clasts in the rock. Porosity is typically

intergranular. Individual voids in the rock generally do not exceed 0.5 mm; some of the larger ones have diameters up to 0.9 mm, and the smaller ones between 0.1 and 0.2 mm. The total porosity of the grainstone-type rock has been estimated at 15 to 20%. The white chalk (samples EGF22 and EGF23) consists of tiny micrite, microsparite and sparite clasts, mostly measuring around 45 µm in diameter. Also very numerous are the



Figure 12: Fossil in the rock. Width of view is 15 cm.

bioclasts represented by different species of planktonic foraminifera, mostly of the *Globigerina* genus, taking up at least 50% of the volume of the rock, which can best be described as biomicrite to biosparite. There is no visible compaction in the rock. Intergranular and especially intragranular porosity are well visible, together estimated at about 30%.

### 3.2.3. COMPLEXOMETRIC TITRATION ANALYSES

We performed 3 complexometric titration analyses (Table 1), according to which more than half of the sandstone in the rock (sample EGF21) is composed of calcite and a good third of dolomite. Due to the heavy micritization of most grains, which usually do not exceed 0.3 mm, alizarin red dye is difficult to distinguish in individual mineral grains in many places. Insoluble residue makes up just under 4%. The chalk rock (samples EGF22 and EGF23) contains over 96% of calcite, a good two percent of dolomite, and less than 2% of insoluble residue.

### 3.3. ROCK RELIEF

Eolian rock features are predominant in the rock relief of the White Desert near Farafra (Figures 13, 14, 15). They are therefore clearly visible in the soft layers of chalk, which are being dissected into the characteristic forms of the karst surface, as they are denuded of the harder layers of sandstone that are disintegrating into sand. The wind whirls this sand around and thus mechanically sculpts the rock features. The geomorphological classification of the karst surface of the Bahariya

and Farafra area divides it into sixteen different types and defines their development (El Aref et al., 2017).

The largest eolian rock features, reaching several meters in size, are: wall niches (Figure 16a); longitudinal notches above the ground; the wall (Figure 16b) and bottom channels (Figure 16c), which have developed into genuine wind gorges in some places (Figure 16d) that dissect the hills. The former are characteristic of the windward slopes of hills, while the latter cut through the hills. Due to their size, rock features are generally dissected by smaller niches, while gorges are dissected by large niches (Figure 16a); yet all of them are also dissected by wind scallops. The large niches higher above the ground are dissected by bottom channels, while their tops are dissected by ceiling channels, which indicate air flowing through the niches. The walls are dissected by large and small cups and channels (Figure 16d), which were formed by eolian erosion between the harder crusts overlying them.

The wind scallops are of different sizes, from meter-sized (Figures 16a, 16d) to decimeter- and centimeter-sized. Sometimes the smaller ones dissect the larger ones and are often connected into a channel (Figure 16e) or a leeward funnel (Figure 16f). The network of scallops clearly reveals the prevailing wind direction (Figure 16g).

On the ground, which is being denuded of the harder layer of rock and is occasionally at least partly covered with sand, rock features form in two main ways. If a steeper windward edge is formed, i.e., when the denuded part of the rock is higher, then a longitudinal notch forms on the edge (Figures 13, 16d) or semi-

circular channel-like cups. Sometimes channels cut through these protrusions (Figure 16c). It seems that at first, when the part of the rock protruding from the sand is low, a gently sloping section is formed, containing shallow channels and wind scallops (Figure 16h),

and a steeper leeward section. If such areas are vaster (Figure 16i), then the surface is more undulating, and sand-filled cups can form on the rock.

The rock pillars (Figure 16j) are carved by the sand-carrying wind out of the parts of the rock which is over-



Figure 13: Hill with wind rock features.



Figure 14: Rock teeth.



Figure 15: Rock pillar.

lain by a harder layer the longest, with the thickness of the layer determining their extensiveness, and out of larger cones. The tallest pillars are mushroom-shaped, as the action of wind and sand is the most intense just above the ground, where it forms longitudinal notches. The water that flowed down the walls or out of smaller cavities (Figure 16k) has caused a crust, typical for this kind of rock and climatic conditions, to form on the surface, which in turn caused the development of the rock relief.

The crusted surfaces generally protrude from the walls, with wind channels deepening around them (Figure 16l). The crust is usually best preserved near the top and also covers the surface of vertical channels. In the sections where eolian erosion is predominant, only smaller crusted surfaces have been preserved. Cups form in the weak sections of the crust and in the sections where the crust has not covered the surface. They are being carved out by the sand-carrying wind.

#### 4. CONCLUSION

The rock relief of wadis in Qara is dominated by dissolution traces made in various carbonate rocks of varying resistance. Its subsediment formation is mostly the result of the sand created by the unconsolidated disintegrated beds transported around by water and wind. Typically, it is made up of subsedimentary rock forms; their distinctive shapes are down to the fact that the sand under which they have formed is being constantly transported around, i.e., they are being regularly uncovered and covered. The unique rock relief of wadi beds features rock forms that can be attributed to ephemeral sand-carrying water streams and the water running down from the

banks. Steep rock parts of water bed that emerge where smaller wadis meet larger ones are also typical. The forms that occur on bare rock are less prominent, as they tend to be occasionally covered by sand at least to some extent. In this way form channels on the steep sections of rock walls as well as higher parts of the rock, and rock forms that are of subsedimentary design when bare.

The sandiest rock beds are co-shaped by water and even more prominently by wind.

In the rock relief of hills, rock cones and pillars, and of the rocky ground of the White Desert near Farafra, eolian rock features prevail. An entire range of rock features

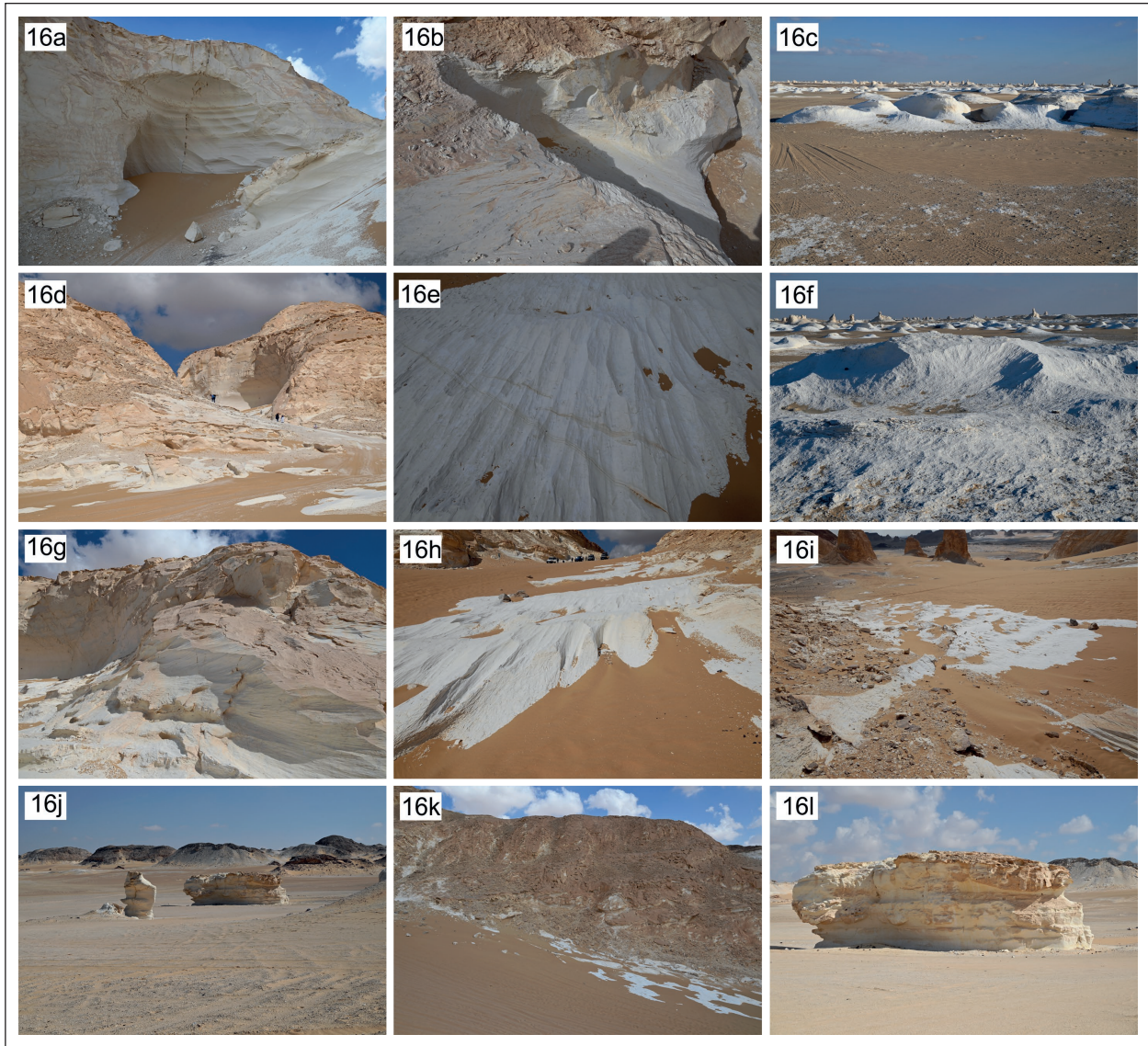


Figure 16: (a) Notch with scallops. Width of view is 20 m, (b) Wall channel. Width of view is 2 m, (c) Floor channels, (d) Wind-shaped gorge, (e) Wind scallops connected in channels. Width of view is 2 m, (f) Wind scallops connected in a funnel-like notch. Width of view is 2 m, (g) Wind scallops on the wall, (h) Wind scallops connected in funnel-like notches and floor channels. Width of view is 8 m, (i) Rock floor dissected by wind rock features. Width of view is 6 m, (j) Rock pillars, (k) Wall dissected by cups and covered by crust, (l) Rock relief of a pillar. Width of view is 10 m.

can be discerned: from large niches and longitudinal notches on the windward side of barriers, channels and gorges crossing the rock barriers, to the smaller scallops dissecting the surface of the rock. The formation of crust on the surface of the rock that is in contact with water is also important for the development of the rock relief. This crust is a trace of the dissolution and hardening of the surface of the rock. At the gaps in the crust, cups are being carved into it by the wind.

The diverse shapes of the rock relief of karst features seem to also be affected by the volume of rainfall, which

is higher in the area of the Qara Oasis, although its distribution and type (e.g., downpour, drizzle) are the decisive factor.

The exposure of the different rock layers provides an insight into the distinct evolution of the karren and the karst surface over various time periods. There are many possibilities for examining the various combinations, however, an intimate knowledge of these phenomena should be the cornerstone for improving our understanding of this type of karst formation process.

## ACKNOWLEDGEMENTS

The authors acknowledge the financial support from the Slovenian Research Agency (research core funding No. P6-0119). Research was supported and included in the framework of projects "Development of research infrastructure for the international competitiveness of the Slovenian rri space RI-SI-EPOS" and "Development of research infrastructure for the international competitiveness of the slovenian rri space RI-SI- LIFEWATCH"; both operations are co-financed by the Republic of Slo-

venia, Ministry of Education, Science and Sport, the European Union, the UNESCO IGCP project No. 661, and the UNESCO Chair on Karst Education.

We wish to thank Mrs. Mojca Škerl for performing the complexometric analyses at the laboratory of the Slovenian National Building and Civil Engineering Institute/Zavod za gradbeništvo Slovenije ZAG, Dimičeva ulica 12, Ljubljana, Slovenia.

## REFERENCES

- Al Farraj Al Ketbi, A., Slabe, T., Knez, M., Gabrovšek, F., Mulec, J., Petrič, M., Zupan Hajna, N., 2014. Karst in Ras Al-Khaimah, northern United Arab Emirates. *Acta carsologica*, 43(1): 23-41. <https://doi.org/10.3986/ac.v43i1.579>
- Audra, P., Bosák, P., Gázquez, F., Cailhol, D., Skála, R., Lisá, L., Jonášová, Š., Frumkin, A., Knez, M., Slabe, T., Zupan Hajna, N., Al Farraj Al Ketbi, A., 2017. Bat urea-derived minerals in arid environment: first identification of allantoin, C<sub>4</sub>H<sub>6</sub>N<sub>4</sub>O<sub>3</sub>, in Kahf Kharrat Najem Cave, United Arab Emirates. *International journal of speleology*, 46(1): 81-92. <https://doi.org/10.5038/1827-806X.46.1.2001>
- Catuneanu, O., Khalifa, M.A., Wanas, H.A., 2006. Sequence stratigraphy of the Lower Cenomanian Baharia Formation, Baharia Oasis, Western Desert, Egypt. *Sedimentary Geology*, 190: 121-137. <https://doi.org/10.1016/j.sedgeo.2006.05.010>
- CEN, 2013. Method of testing cement - Part 2: Chemical analysis of cement. European committee for standardization, 83 pp.
- Coy H.S.C., 1986. Geological map of Egypt, NH 35 SW Siwa, 1:500.000. The Egyptian General Petroleum Corporation, Cairo.
- Coy H.S.C., 1987. Geological map of Egypt, Ng 35 NE Farafra, 1:500.000. The Egyptian General Petroleum Corporation, Cairo.
- Debevec, B., Knez, M., Kranjc, A., Pahor, M., Prelovšek, M., Semeja, A., Slabe, T., 2012. Preliminary study for the adaptation of the "Heaven's Cave" for tourist purposes (Phong Nha-Ke Bang National Park, Vietnam). *Acta carsologica*, 41(1): 115-127. <https://doi.org/10.3986/ac.v41i1.52>
- El Aref, M.M., Hamed, M., Salama, A., 2017. Geomorphological Classification and Zonation of the Surface Karst Landforms of Bahariya-Farafra Region Western Desert, Egypt. *International Journal of Science and Research V 6, I 5*: 956-965.
- El Awady, M.A.M., Abd-Elwahed, A.G., Garamoon, H.K., El Malky, M.G., 2018. Geochemical Assessment of the Quaternary Soil in Siwa Oasis, Western Desert, Egypt. *Journal of Environmental Sciences*, 43(2): 25-45.
- El Marsafawy, S., Bakr, N., Elbana, T., El Ramady, H., 2019. Climate. <https://www.researchgate.net/publication/327141448>. [https://doi.org/10.1007/978-3-319-95516-2\\_5](https://doi.org/10.1007/978-3-319-95516-2_5)
- El Sisi, Z., Hassouba, M., Oldani, M.J., Dolson, J.C., 2002. Ancient Oil, New Energy. International Conference and Exhibition, Field Trip No. 8. British Petrol, Shell, Cairo, 66 p.
- Evamy, B.D., Sherman, D.J., 1962. The application of chemical staining techniques to the study of diagenesis of limestones. *Proc. Geol. Soc. London*, 1599: 102-103.
- Farouk, S., City, N., Abdel Ghany Khalifa, M., El Kom, S., 2010. Facies tracts and sequence development of the Middle Eocene – Middle Miocene successions of the southwestern Qattara Depression, northern Western Desert. *Egypt Freiburger Forschungshefte*, C 536(18): 195-215.
- Fayad, N.H., 2023. Karst landscape morphology of Qarat Umm Al-Saghir Area, Western Desert of Egypt [MsC thesis]. University of Primorska, 187 pp.
- Google Maps, 2023. Google Maps [Map]. <https://maps.app.goo.gl/wyTP3DGCoke2GbJZ7> [Accessed November 26th, 2023].
- Gutiérrez Domech, R., Knez, M. & T. Slabe, 2015. Felo Pérez Mogote (Viñales, Pinar del Río, Cuba): typical shaping of rock surface below dense tropical vegetation. *Acta carsologica*, 44(1): 47-57. <https://doi.org/10.3986/ac.v44i1.680>

- Issawi, B., 1972. Review of Upper Cretaceous-Lower Tertiary stratigraphy in central and southern Egypt. *Bulletin American Association Petroleum Geologists*, 56:1448-1463. <https://doi.org/10.1306/819A40F2-16C5-11D7-8645000102C1865D>
- Khalil, M., Elharairy, M., Atta, E., Aboelkhair, H., 2021. Evaluation of salts in salt pans, Siwa Oasis, Egypt. *Arabian Journal of Geosciences*, 14(770): 2-11. <https://doi.org/10.1007/s12517-021-07060-z>
- Knez, M., Liu, H., Slabe, T., 2010: High Mountain Karren in Northwestern Yunnan, China. *Acta carsologica*, 39(1): 103-114. <https://doi.org/10.3986/ac.v39i1.116>
- Knez, M., Liu, H. & T. Slabe, 2012: Major stone forest, litomorphogenesis and development of typical shilin (Yunnan, China). *Acta carsologica*, 41(2/3): 205-218. <https://doi.org/10.3986/ac.v41i2-3.558>
- Knez, M., Liu, H., T.Slabe, 2022. Clustered stone forest in Pu Dou Chun (Yunnan, China). *Acta carsologica*, 51(1): 47-63. <https://doi.org/10.3986/ac.v51i1.10688>
- Knez, M., Otoničar, B., Slabe T., 2003. Subcutaneous stone forest (Trebnje, Central Slovenija). *Acta carsologica*, 32(1): 29-38. <https://doi.org/10.3986/ac.v32i1.362>
- Knez, M., Rubinić, J., Slabe, T., Šegina, E., 2015. Karren of the Kamenjak hum (Dalmatian Karst, Croatia): from the initial dissection of flat surfaces by rain to rocky points. *Acta carsologica*, 44(2): 191-204. <https://doi.org/10.3986/ac.v44i2.1546>
- Knez, M., Ruggieri, R., Slabe, T., 2019. Karren above Customaci (Sicily, Italy). In: *The European Bi-annual Conference on the Hydrogeology of Karst and Carbonate Reservoirs, Eurokarst, The European Conference on Karst Hydrogeology and Carbonate Reservoirs, Besançon, France, 98.*
- Knez, M., Slabe, T., Panisset Travassos, L.E., 2011. Karren on laminar calcarenitic rock of Lagoa Santa (Minas Gerais, Brazil). *Acta carsologica*, 40(2): 357-367. <https://doi.org/10.3986/ac.v40i2.19K>
- Knez, M., Slabe, T., Trajanova, M., Akimova, T., Kalmykov, I., 2020. The karren peeling off on marbles in Altai (Altai Republic, Russian Federation). *Acta carsologica*, 49(1): 11-38. <https://doi.org/10.3986/ac.v49i1.7197>
- Knez, M., Slabe, T., Urushibara-Yoshino, K., 2017. Lithology, rock relief and karstification of Minamidaito Island (Japan). *Acta carsologica*, 46(1): 47-62. <https://doi.org/10.3986/ac.v46i1.2022>
- Munsell Rock-Color Chart, 2009. *Geological Rock-Color Chart*. Munsell Color, Grand Rapids, MI, USA.
- Plyusnina, E.E., Emad S., Sallam, D., Ruban, A., 2016. Geological heritage of the Bahariya and Farafra oases, the central Western Desert, Egypt. *Journal of African Earth Sciences*, 116: 151-159. <https://doi.org/10.1016/j.jafrearsci.2016.01.002>
- Said, R., 1990. *The geology of Egypt*. A.A. Balkema, Rotterdam, 734 pp.
- Slabe, T., Hada, A., Knez, M., 2016. Laboratory modeling of karst phenomena and their rock relief on plaster, subsoil karren, rain flutes karren and caves. *Acta carsologica*, 45(2): 187-204. <https://doi.org/10.3986/ac.v45i2.4623>
- Slabe, T., Knez, M., Drame, L., 2021. Development model of rock relief on thick horizontal and gently sloping rock strata exposed to rain. *Acta carsologica*, 508(2/3): 209-230, ilustr. ISSN 0583-6050. <https://doi.org/10.3986/ac.v50i2-3.9308>
- Slaughter, B.H., Thurmond, J.T., 1974. A lower cenomanian (Cretaceous) Ichthyofauna from the bahariya formation of Egypt. *Annals of the Geological Survey of Egypt*, 4: 25-40.
- Stromer, E., 1936. *Ergebnisse der Forschungsreisen Prof. E. Stromers in den Wusten Agyptens. VII. Bahariya Kessel und Stufe mit deren Fauna und flora. Eine erganzende usammenfassung. Abhandl. Konig. Bayer. Akad. Wiss. Math. Phys. Kl. 26(3): 259-292.*
- Thabet, M.A., Abdel Hady, A.A., Abd El Kawy, W.A.M., EL-Nahry, A.H., 2013. Study of land resources at Siwa oasis using remote sensing and GIS techniques. *Journal of Soil Sciences and Agricultural Engineering*, 4(8): 757-773. <https://doi.org/10.21608/js-sae.2013.52077>
- Zaki, A., Abdel-Fattah, M., Kora, A., Salah, N.A., 2013. Facies architecture and depositional development of Middle Miocene carbonate strata at Siwa Oasis, Northwestern Egypt. *Facies. International Journal of Paleontology, Sedimentology and Geology*, 59: 505-528. <https://doi.org/10.1007/s10347-012-0332-2>